

# Stability exchanges between periodic orbits in a Hamiltonian dynamical system

Anders B. Eriksson

*Institute of Theoretical Physics, Chalmers University of Technology, S-412 96 Göteborg, Sweden*

Per Dahlqvist

*Mechanics Department, Royal Institute of Technology, S-100 44 Stockholm, Sweden*

(Received 25 September 1992; revised manuscript received 28 October 1992)

Exchange of stability between periodic orbits of the same winding number is observed in a one-parameter family of quartic potentials. We use numerical simulations to study the exchanges that occur between two values of the parameter for which the system is integrable. The relevance for the survival of Kolmogorov-Arnold-Moser tori is briefly discussed and parallels are drawn to a similar phenomenon earlier observed for area-preserving maps.

PACS number(s): 05.45.+b

## I. INTRODUCTION

In this article we report a remarkable phenomenon that we have observed in a system described by the Hamiltonian

$$H = \frac{1}{2}(p_x^2 + p_y^2) + \frac{1}{4}(x^4 + y^4) + \frac{\epsilon}{2}x^2y^2. \quad (1)$$

At  $\epsilon = 0$  the system is integrable and the trajectories are marginally stable and form so-called invariant circles. According to linear theory a typical trajectory grows stable (or unstable) linearly in  $\epsilon$ . In numerical simulations, however, the trajectories turn out to oscillate between stability and instability even for very small values of  $\epsilon$ , indicating a rapid breakdown of the linear theory. The existence of the invariant circles is in some sense prolonged by the stability oscillations since the trajectories are forced to remain almost marginally stable.

During the last decade, a considerable fraction of the work on Hamiltonian chaotics has been centered on the question: when does the last invariant circle in the standard map disappear [1–5]. The reason for studying maps rather than Hamiltonian flows themselves is often a question of computational economy. However, Hamiltonian flows are interesting on their own, since we often do not know if discrete mappings really represent generic behavior of the continuous systems. This serves as a motivation for studying the phenomenon described above, although a similar phenomenon has already been observed for area-preserving maps.

As background and for defining some useful concepts let us begin by briefly discussing maps. The standard map is defined by

$$\begin{aligned} \theta_{n+1} &= \theta_n + r_n - f(\theta_n), \\ r_{n+1} &= r_n - f(\theta_n), \end{aligned} \quad (2)$$

where  $f(\theta) = (K/2\pi)\sin(2\pi\theta)$ . Since  $f(\theta)$  is periodic, one may regard the map as acting on a cylinder. If the limit  $\Omega = \lim_{n \rightarrow \infty} (\theta_n - \theta_0)/n$  exists,  $\Omega$  is defined as the winding number. Periodic points with a rational winding number,  $\Omega = m/n$ , typically lie in a chain consisting of an alternating sequence of hyperbolic and elliptic

periodic points. The elliptic points are surrounded by islands with quasiperiodic motion, which in turn are surrounded by chaotic motion. If  $\Omega$  is irrational the corresponding iterates of the map lies on an invariant circle. The existence of invariant circles with irrational winding numbers is ensured by the Kolmogorov-Arnold-Moser (KAM) theorem, provided the perturbation is *sufficiently* weak. However, numerical experience shows that irrational curves survive much larger perturbations than the rigorously established bounds.

It is generally believed that the last invariant circle to be destroyed as a perturbation is increased, has the inverse golden mean,  $\omega = (\sqrt{5} - 1)/2$ , as a winding number. There is numerical evidence [2] that this circle exists when  $K < K_c \approx 0.971\,635$ . Invariant circles of the standard map and maps of similar topology form unpenetrable barriers for the chaotic trajectories of the map and each one of the invariant circles divide the cylinder into two separate halves. When  $K > K_c$  the last such barrier disappears and one says that connected stochasticity occurs. This transition is most easily studied by means of the residue criterion [2]. The basic idea is that any irrational may be approximated by rationals to any degree of accuracy. The fastest converging sequence of approximating rationals  $m_N/n_N$ ,  $N = 1, 2, \dots$  is given by continued-fraction expansions. One now studies the sequence of residues,  $R_N \equiv [2 - \text{Tr}(M_N)]/4$ , where  $M_N$  are the stability matrices for the corresponding periodic orbits. If the invariant circle exists, then  $R \rightarrow 0$  as  $N \rightarrow \infty$ , but when it does not exist  $R \rightarrow \pm\infty$ .

If the map is generalized to a two-parameter system [6, 7], one could expect the critical point  $K = K_c$  to be generalized to a smooth critical line in the parameter plane. But what one really finds in this, and in related systems, is a fractal set of cusps [6–10]. Associated with the cusp structure one observes a peculiar phenomenon. It seems as if the elliptic and hyperbolic periodic points in a chain sometimes suddenly changes identity. Assuming that we move along a curve in the parameter plane, a closer inspection yields that at some parameter value the elliptic (hyperbolic) point bifurcates into one hyperbolic (ellip-

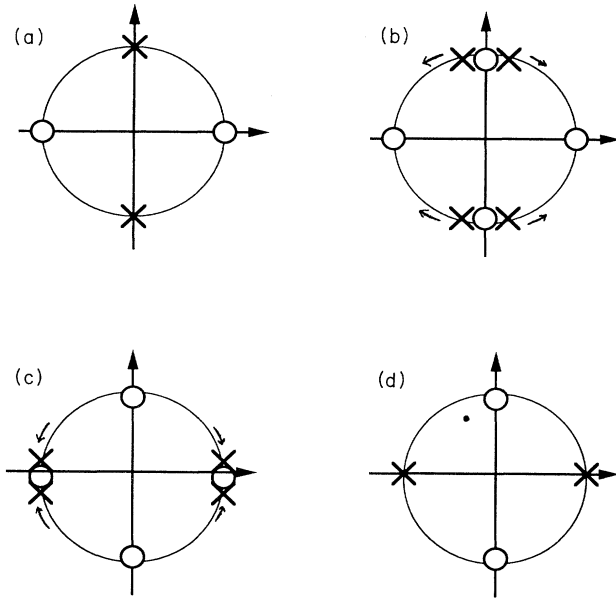


FIG. 1. An example of how a stability exchange with a hyperbolic exchange orbit in principle may look. The hyperbolic orbits on a symmetry axis (a) change to elliptic ones emitting two hyperbolic periodic orbits each (b). These start to move to the nearby elliptic orbits (c) and change them to hyperbolic (d).

tic) and two elliptic (hyperbolic). These newly created cycles start to move to the nearby hyperbolic (elliptic) point and change this to an elliptic (hyperbolic) point [7, 11]. In Fig. 1 it is shown how such an exchange, with a hyperbolic exchange orbit, may look. This process (which very much resembles particle exchange in quantum-field theories) is important for the recurrence of the nearby KAM circle [12], since during the process the residue of the nearby periodic orbit will remain close to 0.

## II. STABILITY EXCHANGES IN A DYNAMICAL SYSTEM

We now turn to the dynamical system described by the Hamiltonian in Eq. (1). The Hamiltonian has the following symmetries:

(1) The potential is invariant under the symmetry group  $C_{4v}$ . When  $\epsilon = 1$ , the symmetry degenerates to the full  $O(2)$  rotation symmetry.

(2) The potential is invariant under the parameter exchange  $\epsilon \rightarrow (3 - \epsilon)/(1 + \epsilon)$  followed by a  $\pi/4$  rotation of the configuration plane and a simple rescaling of the length scale.

(3) The system is symmetric under time reversal since the Hamiltonian is even in the momenta.

When  $\epsilon = 0$  (and equivalently  $\epsilon = 3$ ) the system is integrable due to separability and when  $\epsilon = 1$  due to the rotational symmetry. In the limit  $\epsilon \rightarrow \infty$  (and equivalently when  $\epsilon \rightarrow -1$ ), we obtain the frequently studied  $x^2y^2$  model where almost the entire phase space is filled by chaotic trajectories, c.f. Ref. [13]. The Hamiltonian

is such that any rescaling of energy can be obtained by rescaling time and length, and it is thereby sufficient to study just one energy. We always use  $E = 0.5$  in our numerical simulations.

### A. The integrable case $\epsilon = 0$

In this case the system is separable and we may transform the canonical pairs  $(x, p_x)$  and  $(y, p_y)$  to action-angle variables  $(I_x, \theta_x)$  and  $(I_y, \theta_y)$ . The Hamiltonian now reads

$$H = \gamma(I_x^{4/3} + I_y^{4/3}), \quad (3)$$

where  $\gamma$  is a constant involving an elliptic integral.

Each choice of  $I_x, I_y$  corresponds to an invariant torus, and the angular frequencies are given by

$$\dot{\theta}_i = \frac{\partial H}{\partial I_i} = \gamma \frac{4}{3} I_i^{1/3}, \quad i = x, y. \quad (4)$$

A torus is periodic whenever  $\Omega = \dot{\theta}_x/\dot{\theta}_y = m_x/m_y$ , where  $m_x$  and  $m_y$  are integers. This means that the orbit closes onto itself after  $m_x$  oscillations in the  $x$  direction and  $m_y$  in the  $y$  direction. We will refer to  $m_x$  and  $m_y$  as the *resonance numbers*.

An area-preserving map  $(x_{n+1}, p_{x,n+1}) = T(x_n, p_{x,n})$  is defined in the usual way by the Poincaré section  $y = 0, p_y > 0$ . The periodic (or resonant) torus defined by the numbers  $m_x, m_y$  cut the Poincaré section along the curve

$$\frac{1}{2}p_x^2 + \frac{1}{4}x^4 = E \frac{m_x^4}{m_x^4 + m_y^4}. \quad (5)$$

Any point along this curve is a fixed point under the map  $T^{m_y}$ .

### B. Small $\epsilon$

When the perturbation is *small* the usual chain of islands will appear along the curve (5), cf., e.g., Refs. [14, 15]. By the following argument one immediately realizes that there are always periodic points (i.e., fixed points under  $T^{m_y}$ ) on the  $p_x$  and  $x$  axis. Suppose there is a periodic point at  $(x, p_x)$ . Then there are, for symmetry reasons, periodic points of the same kind (hyperbolic or elliptic) at  $(-x, p_x)$ ,  $(x, -p_x)$ , and  $(-x, -p_x)$ . Between any two of them there has to be an odd number of periodic points, and one of these has to lie on the axis, again for symmetry reasons.

Let us now assume  $\epsilon$  to be *small* and *positive*. One may then show, by first-order perturbation theory (cf., e.g., Ref. [14]), that there are exactly one hyperbolic (unstable) and one elliptic (stable) orbit around any rational torus, thus regarding orbits related by symmetries as one and the same. An exception is the elliptic orbit  $(m_x, m_y) = (0, 1)$ , which has no hyperbolic partner. From first-order perturbation theory we find the following simple rules:

(1) The orbit with a periodic point on the  $x$  axes is

stable if  $m_x$  is odd and unstable if  $m_x$  is even.

(2) The orbit with a periodic point on the  $p_x$  axes is stable if  $m_x + m_y$  is odd and unstable if  $m_x + m_y$  is even.

We now want to study numerically how the stability of these orbits vary with  $\epsilon$ . Since we know the approximate position of the fixed points it is straightforward to exactly localize them with a two-dimensional Newton-Raphson algorithm, and compute their residues for different perturbation strengths. The equations of motion are integrated with a fourth-order Runge-Kutta method using a precision of  $10^{-10}$  (in some cases  $10^{-7}$  is sufficient). These stable and unstable orbits will be called  $(m_x, m_y)s$  and  $(m_x, m_y)u$ , respectively. Due to the  $x \leftrightarrow y$  symmetry we only consider the resonances  $m_x \leq m_y$  in the following.

We find that generally, if  $m_x > 1$ , the orbits oscillate between being hyperbolic and elliptic and that first-order perturbation theory breaks down at extremely small perturbations. The residue for the  $(3, 5)$  resonance as a function of  $\epsilon$  is displayed in Fig. 2. In the figure it looks as if the  $(3, 5)s$  and the  $(3, 5)u$  crosses the  $R = 0$  axis at the same  $\epsilon$  value. A closer inspection reveals that the exchange of stabilities is mediated by an exchange orbit in the way described above. For the  $(2, 3)$  resonance an elliptic exchange orbit is born by the  $(2, 3)s$  at  $\epsilon \approx 0.0554788$ , moves quickly along what used to be an invariant curve, and is absorbed by the  $(2, 3)u$  at  $\epsilon \approx 0.0554822$ . The  $(2, 3)s$  and  $(2, 3)u$  orbits remain on the axis, as they have to, and move very little along the axis during the exchange. The  $\epsilon$  values for the exchanges for a number of resonances are displayed in Table I. The exchanges take place during extremely small intervals in  $\epsilon$  so the accuracy in the table holds for both  $(m_x, m_y)s$  and  $(m_x, m_y)u$ . Generally the residue is very symmetric around zero and in the following discussion we will often neglect the small asymmetry.

Empirically we find that the number of stability exchanges is equal to  $m_x - 1$ , and that they all occur at positive  $\epsilon$ . We also calculate the slope of  $R(\epsilon)$  to first-order in  $\epsilon$  so we can recognize the region where first-order theory holds and no further crossings are to be found.

Why does the exchange phenomenon only occur for

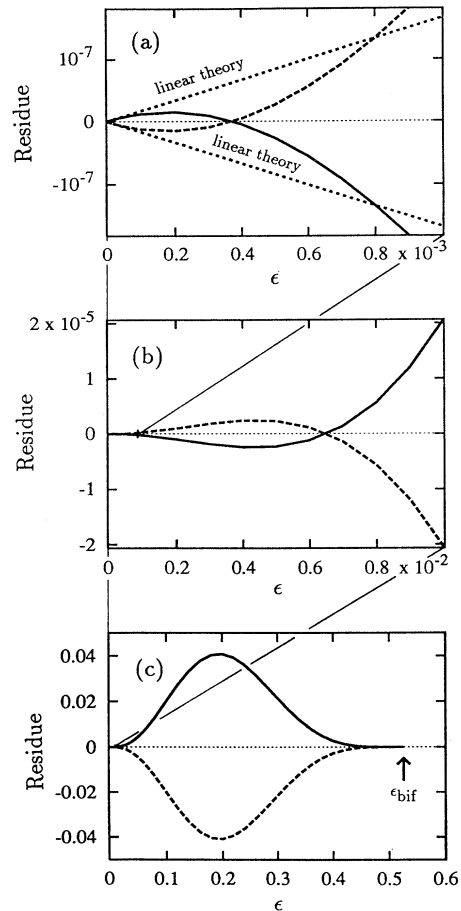


FIG. 2. Residues for the two orbits  $(3, 5)s$  and  $(3, 5)u$ . The approximation given by linear theory is also plotted in (a).

$\epsilon > 0$ ? In the range  $0 > \epsilon > -1$  the system changes, in some sense, monotonously from integrability to chaos. But in the range  $0 < \epsilon < 1$  we move from one integrable case to another (the chaotic fraction of a Poincaré plot

TABLE I. Approximate values for the crossings of the  $R = 0$  axis, where “-” denotes possible crossings that are not resolved. The two rightmost columns give the points where the orbits bifurcate with  $(0, 1)$  according to numerical simulations and theory [Eq. (9)].

$m_x$	$m_y$	$\epsilon_{\text{cross}}$	$\epsilon_{\text{bif}}$	
			Num.	Theor.
2	3	0.0005548	0.63	0.632
2	5	0.00049	0.24	0.245
2	7	0.0001	0.127	0.127
3	4	0.0011	0.76	0.764
3	5	0.00037	0.52	0.526
3	7	(0.0001)	0.28	0.279
4	5	0.0003	0.83	0.838
4	7	-	0.48	0.481
5	6	-	0.88	0.883
5	7	-	0.71	0.708

thus never exceeds 10% [16]). May the exchange phenomenon be related to this transition? We will see that this transition will mean a major reorganization of periodic orbits because of the change of symmetry groups. Let us first briefly discuss the integrable case  $\epsilon = 1$ .

### C. The integrable case $\epsilon = 1$

Due to the rotational symmetry the angular momentum,  $L = r^2\dot{\phi}$ , where  $(x, y) = r[\cos(\phi), \sin(\phi)]$ , is now a constant of motion. The Hamiltonian reads

$$H = \frac{1}{2}p_r^2 + \frac{1}{2}\frac{L^2}{r^2} + \frac{1}{4}r^4, \quad (6)$$

where  $p_r = \dot{r}$ . The Poincaré cut  $y = 0$  means  $\phi = 0$  (if  $x > 0$ ), so in the surface of section we have  $x = r$  and  $p_x = p_r$ . The invariant curves under the map are given by

$$\frac{1}{2}p_x^2 + \frac{1}{2}\frac{L^2}{x^2} + \frac{1}{4}x^4 = E, \quad (7)$$

as illustrated in Fig. 3(c). In the center of the invariant

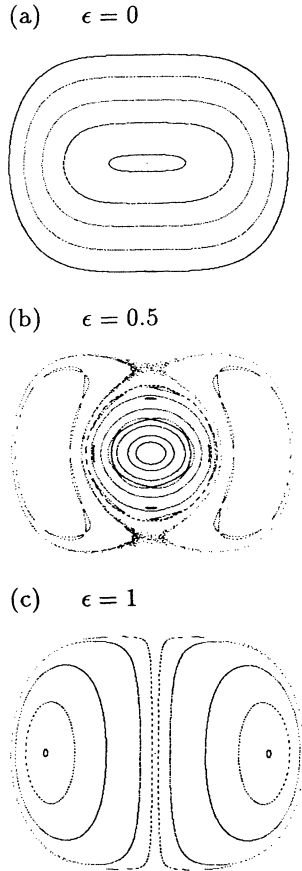


FIG. 3. The Poincaré plot at the two parameter values ( $\epsilon = 0$  and  $\epsilon = 1$ ) for which the system is integrable and at one intermediate value ( $\epsilon = 0.5$ ).

curves lies the  $(1,1)s$  orbit with no oscillations in the radial directions and with  $L = L_{\max} = (\frac{2}{3})^{3/4}\sqrt{2E}$ . When  $L = 0$  all orbits have to go through the origin and their periodic points thereby lie on the line  $x = 0$ .

### D. The transition $0 \leq \epsilon \leq 1$

For general  $\epsilon$  there are rigorous results, due to Yoshida [17], concerning the two orbits along the lines  $y = 0$  and  $y = x$ . According to the previously defined coding (for the small positive  $\epsilon$  case) these are the  $(0, 1)$  and  $(1, 1)u$ , respectively. They exist for all  $\epsilon$  values and the traces of the stability matrices are given by [17]

$$\begin{aligned} (y = 0) \text{Tr}(M) &= 2\sqrt{2} \cos(\sqrt{1 + 8\epsilon}\frac{\pi}{4}), \\ (y = x) \text{Tr}(M) &= 2\sqrt{2} \cos[\sqrt{1 + 8(3 - \epsilon)/(1 + \epsilon)}\frac{\pi}{4}]. \end{aligned} \quad (8)$$

We note that in the range  $0 < \epsilon < 1$  the first of them is stable and the second unstable and when  $\epsilon = 0$  and  $\epsilon = 1$  they are marginally stable. The invariant line  $x = 0$  in the Poincaré section in the  $\epsilon = 1$  case (corresponding to  $L = 0$ ) will be split up into the periodic points of these two orbits when  $\epsilon$  is slightly changed.

We also see that all periodic orbits in the  $\epsilon \approx 1$  case with  $L \neq 0$  have the same winding number as the  $(1, 1)s$  orbit (i.e., the simple rotation) with respect to the Poincaré section  $y = 0$ . Indeed, they are found to be born by higher-order bifurcations (or  $n$ -uplings, cf. [18]) from  $(1, 1)s$ . This orbit also exists for any  $\epsilon$  and in the case  $\epsilon = 1$  it is the one with  $L = L_{\max}$ . All the other orbits from the  $\epsilon \approx 0$  case have disappeared by bifurcating with the  $(0, 1)$  orbit, and these higher-order bifurcations take place when  $\text{Tr}(M) = 2 \cos(\pi m_x/m_y)$ . We will refer to these bifurcations as *prunings* in the following. From Eq. (8) we can calculate exactly when this happens,

$$\sqrt{2} \cos\left(\sqrt{1 + 8\epsilon_{\text{bif}}}\frac{\pi}{4}\right) = \cos\left(\frac{m_x \pi}{m_y}\right). \quad (9)$$

This is found to be consistent with the numerical findings, cf. Table I. The phase-space plots in Fig. 3 illustrate the transition from  $\epsilon = 0$  to  $\epsilon = 1$ . It is seen how the island around the origin [the periodic point of  $(0, 1)$ ] is shrinking as  $\epsilon$  increases, whereas the islands around the fixed points of  $(1, 1)s$  are growing.

The behavior of the residue  $R(\epsilon)$  close to the bifurcation point  $\epsilon_{\text{bif}}$  is given by  $R(\epsilon) = C(m_x, m_y)(\epsilon_{\text{bif}} - \epsilon)^{m_y}$ . This result may be obtained by analyzing the normal form, taking care of the symmetries of the problem, as in Ref. [19], and it also agrees with our numerical data. We will now see that the residue, as a function of  $\epsilon$ , is well approximated by a polynomial. We therefore make the ansatz

$$R(\epsilon) = \left(1 - \frac{\epsilon}{\epsilon_{\text{bif}}}\right)^{m_y} k \epsilon \prod_{i=1}^{m_x-1} \left(1 - \frac{\epsilon}{\epsilon_{\text{cross}, i}}\right), \quad (10)$$

where the factor  $k$  is obtained from first-order theory,  $\epsilon_{\text{cross}, i}$  is the value for the  $i$ th crossing which is obtained numerically, and  $\epsilon_{\text{bif}}$  is given by Eq. (9). We see from Fig. 4 that this simple formula surprisingly well describes

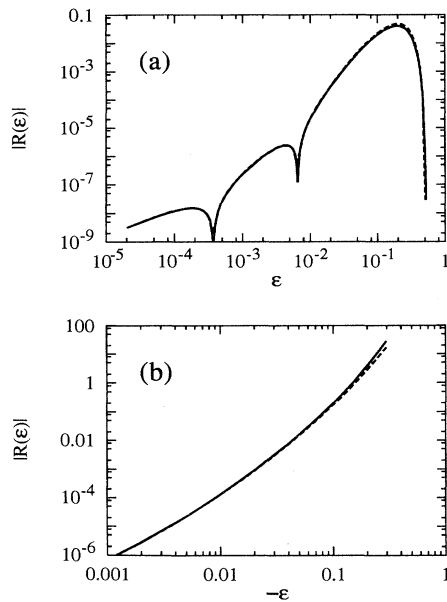


FIG. 4. The modulus of the residue as a function of  $\epsilon$  for the  $(3, 5)u$  orbit (full line) plotted together with the modulus of the polynomial given by Eq. (10) (dashed line). The residue of the  $(3, 5)s$  orbit is not plotted since its deviation from the  $(3, 5)u$  orbit is negligible compared to the deviation from the polynomial.

Fig. 4 that this simple formula surprisingly well describes the behavior of  $R(\epsilon)$  both for positive and negative  $\epsilon$ . For negative  $\epsilon$  the agreement is good, at least as long as the fraction of phase space covered by chaotic trajectories is still small, cf. Ref. [16]. This means the knowledge of the behavior at small  $\epsilon$  (that is  $k$  and  $\epsilon_{\text{cross},i}$ ) yields a very good value for the constant  $C(m_x, m_y)$  describing

the behavior close to the pruning. This indicates that the stability exchanges and the pruning are intimately connected. There is another circumstance supporting this connection. The number of stability exchanges occurring for the  $(m_x, m_y)$  resonance is  $m_x - 1$ , i.e., equal to the number of resonances with period  $m_y$  that are killed by bifurcation before the resonance  $(m_x, m_y)$  itself, although the stability exchanges occur well before these bifurcations.

### III. CONCLUDING REMARKS

The early breakdown of perturbation theory for this system may be understood as follows. When analyzing the motion around a resonant torus for small  $\epsilon$  one expands the perturbation into a Fourier series. All Fourier terms except the resonant one are averaged away for small enough  $\epsilon$ . But, the sequence of Fourier coefficients decreases exponentially. This means that the terms that are assumed to disappear through the averaging procedure are generally much bigger than the resonant term itself, and first-order theory thereby breaks down very early.

In this paper we have argued that there is a connection between the exchange of stabilities and the transition from one integrable subcase to another. This coherent behavior over orders of magnitude in the perturbation illustrates well the difficulties of perturbation theory and the problem of establishing bounds for the survival of KAM tori. We find it likely that similar exchanges occur around  $\epsilon = 1$  as well as for many other systems.

### ACKNOWLEDGMENT

We would like to thank Jukka Ketoja for introducing us to his work on the generalized standard map.

- 
- [1] B. V. Chirikov, Phys. Rep. **52**, 263 (1979).
  - [2] J. M. Greene, J. Math. Phys. **20**, 1183 (1979).
  - [3] R. S. MacKay, Physica D **7**, 462 (1983).
  - [4] J. M. Mather, Erg. Theor. Dyn. Sys. **4**, 301 (1984).
  - [5] R. S. MacKay and I. C. Percival, Commun. Math. Phys. **98**, 469 (1985).
  - [6] J. A. Ketoja and R. S. MacKay, Physica D **35**, 318 (1989).
  - [7] J. Wilbrink, Physica D **26**, 358 (1987).
  - [8] J. A. Ketoja, Phys. Rev. A **42**, 775 (1990).
  - [9] J. Wilbrink, Nonlinearity **3**, 567 (1990).
  - [10] H. Urbschat, Phys. Rev. Lett. **54**, 588 (1985).
  - [11] R. C. Black and I. I. Satija, Phys. Rev. Lett. **65**, 1 (1990).
  - [12] B. Hu, J. Shi, and S.-Y. Kim, J. Stat. Phys. **62**, 631 (1991).
  - [13] P. Dahlqvist and G. Russberg, Phys. Rev. Lett. **65**, 2837 (1990).
  - [14] M. C. Gutzwiller, *Chaos in Classical and Quantum Mechanics* (Springer-Verlag, New York, 1990).
  - [15] *Hamiltonian Dynamical Systems*, edited by R. S. MacKay and J. D. Meiss (Hilger, Bristol, 1987).
  - [16] N. Caranicolas and C. Vozikis, Celest. Mech. **40**, 35 (1974).
  - [17] H. Yoshida, Celest. Mech. **32**, 73 (1984).
  - [18] J. M. Greene, R. S. MacKay, F. Vivaldi, and M. J. Feigenbaum, Physica D **3**, 468 (1981).
  - [19] M. A. M. de Aguiar, C. P. Malta, M. Baranger, and K. T. R. Davies, Ann. Phys. (N.Y.) **180**, 167 (1987).